Author Manuscript

Author Manuscript

Author Manuscript

Author Manuscript

HHS Public Access

Author manuscript

Nat Immunol. Author manuscript; available in PMC 2020 August 17.

Published in final edited form as:

Nat Immunol. 2020 April ; 21(4): 412–421. doi:10.1038/s41590-020-0607-7.

Developmental plasticity allows outside-in immune responses by resident memory T cells

Raissa Fonseca[1,5,+], **Lalit K Beura**[1,6,+], **Clare F Quarnstrom**[1,+], **Hazem E Ghoneim**[2,7], **Yiping Fan**[3], **Caitlin C Zebley**[2], **Milcah C Scott**[1], **Nancy J Fares-Frederickson**[1], **Sathi Wijeyesinghe**[1], **Emily A Thompson**[1], **Henrique Borges da Silva**[4], **Vaiva Vezys**[1], **Benjamin Youngblood**[2], **David Masopust**[1,*]

[1]Department of Microbiology and Immunology, Center for Immunology, University of Minnesota Medical School, Minneapolis MN, 55455. USA.

[2]Department of Immunology, St. Jude Children's Research Hospital, Memphis, TN 38105. USA.

[3]The Department of Computational Biology, St. Jude Children's Research Hospital, Memphis, TN 38105, USA

[4]Department of Laboratory Medicine and Pathology, Center for Immunology, University of Minnesota Medical School, Minneapolis, MN, 55455. USA.

[5]Present address-Department of Microbiology and Immunology, The University of Melbourne and The Peter Doherty Institute for Infection and Immunity, Melbourne, VIC, Australia.

[6]Present address-Department of Molecular Microbiology and Immunology, Brown University, Providence, RI, 02912. USA.

[7]Present address-Department of Microbial Infection and Immunity, College of Medicine, the Ohio State University, Columbus, OH 43210, USA.

Abstract

Central memory T (T_{CM}) cells patrol lymph nodes and perform conventional memory responses upon re-stimulation: proliferation, migration, and differentiation into diverse T cell subsets while also self-renewing. Resident memory T (T_{RM}) cells are parked within single organs, share properties with terminal effectors, and contribute to rapid host protection. We observed that reactivated T_{RM} cells rejoined the circulating pool. Epigenetic analyses revealed that T_{RM} cells align closely with conventional memory T cell populations, bearing little resemblance to recently activated effectors. Fully differentiated T_{RM} cells isolated from small intestine epithelium exhibited the potential to differentiate into T_{CM}, T_{EM}, and T_{RM} cells upon recall. Ex-T_{RM} cells,

Users may view, print, copy, and download text and data-mine the content in such documents, for the purposes of academic research, subject always to the full Conditions of use:http://www.nature.com/authors/editorial_policies/license.html#terms

*Corresponding author.

+Equal contribution

Author Contributions

RF, LKB, CFQ, NJF-F, SW, EAT and HBS performed and analyzed experiments; HEG and YF performed and analyzed WGBS; CCZ, MCS conducted bioinformatics analysis; RF, LKB, CFQ, NJF, VV, BY, and DM designed experiments and prepared the manuscript; DM was responsible for research supervision, coordination and strategy.

Competing interests

The authors declare no competing interests.

Author Manuscript Author Manuscript Author Manuscript Author Manuscript

former intestinal T_{RM} that rejoined the circulating pool, heritably maintained a predilection for homing back to their tissue of origin upon subsequent reactivation and a heightened capacity to re-differentiate into T_{RM} cells. Thus, T_{RM} cells can rejoin the circulation but are advantaged to re-form local T_{RM} when called upon.

Introduction

Antigen-specific $CD8^+$ T cells protect mammalian hosts from intracellular infections. The extensive repertoire of T cells needed to protect the host from a variety of foreign antigens limits naive cell clonal abundance[1]. Naive T cell recirculation is thus restricted to secondary lymphoid organs (SLOs), facilitating its encounter with cognate antigen presented by antigen presenting cells[2]. After activation, $CD8^+$ T cells proliferate to become numerically relevant and migrate outwards to nonlymphoid tissues to seek infected cells[3]. After a return to homeostasis, clonally expanded memory T cells (relative to their naive predecessors) are left behind, and persist in lymphoid and nonlymphoid tissues, providing enhanced protection against subsequent infections[4–8].

Memory T cells are functionally specialized and often partitioned into putatively discrete subsets with uncertain developmental relationships[9–13]. Like naive T cells, T_{CM} recirculate amongst lymph nodes (LNs), and when reactivated, fulfill the canonical properties of self-driven expansion, differentiation into diverse T cell types, and acquisition of new homing properties[10,14]. Effector memory T cells (T_{EM}) are a heterogeneous population that patrols blood[12,15]. Immune surveillance of nonlymphoid tissues is mostly assumed by T_{RM} that park within tissues during the effector phase of the response[16–19]. T_{RM} act as first responders against local reinfection and accelerate pathogen control[7,20,21]. Indeed, they share many properties with recently activated effector T cells, supporting that they may constitute a terminally differentiated population[11,22,23].

In summary, in the event of reinfection at barrier sites, immune organisms have an opportunity for local control by T_{RM} cells. If that immunity fails, the recall response can be modeled as a faster recapitulation of a primary response, originating in LNs, but being driven by T_{CM} instead of naive T cells. This can be visualized as an ‘inside-out’ model, where immune responses originate inside LNs and migrate out toward peripheral tissues. This model fails to capture the observation that T_{RM} cells proliferate[24,25] and contribute to durable expansion of the local memory population in response to antigen restimulation[26]. Here, we show that re-stimulated T_{RM} cells undergo retrograde migration, exhibit developmental plasticity, join the circulation, give rise to T_{CM} and T_{EM} cells, yet retain biased homing and T_{RM} differentiation potential. Collectively, this supports a new ‘outside-in’ model of protective immunity.

Results

Local reactivation of T_{RM} precipitates egress to circulation

To assess whether local reactivation of T_{RM} cells precipitates egress to circulation, we generated C57BL/6J mice that contained $CD90.1^+$ OT-I T_{RM} cells within skin through

Author Manuscript Author Manuscript Author Manuscript Author Manuscript

Vesicular stomatitis virus expressing ovalbumin (VSVova) viral infection (OT-I chimeras, see Methods). After viral clearance, skin was engrafted onto infection matched CD45.1$^+$ OT-I immune chimeric C57BL/6J mice. 30 days later, we reactivated T_{RM} cells within the skin graft by injecting SIINFEKL peptide, which is recognized by OT-I T cells (Fig. 1a). 2–3 weeks later, displaced residents were observed within the draining lymph node, and circulating T_{CM} and T_{EM} cells were observed in distant lymph nodes (Fig. 1b), suggesting that reactivated T_{RM} may give rise to T_{RM}, T_{EM}, and T_{CM} cells.

To further test T_{RM} retrograde migration and plasticity, we depleted CD90.1$^+$ circulating T_{EM} and T_{CM} from OT-I chimeras via titrated injection of depleting anti-CD90.1 antibody (which depletes circulating cells while sparing many T_{RM} cells[27]). As a control, these mice were seeded with an independent population of undepleted CD90.1$^-$CD45.1$^+$ circulating OT-I memory T cells. Mice were then challenged with SIINFEKL peptide in the skin (Fig. 1c). 10 days later, CD90.1$^+$ OT-I appeared in the blood, and many of these cells transiently retained a phenotype that distinguish skin T_{RM} from circulating T_{CM} and T_{EM} (CD103$^+$ CD49a^{hi}Ly6C^{lo}) and exhibited other properties shared by T_{RM} and long lived T_{EM}, including lack of KLRG1 and CD62L expression (Fig. 1d and e). We performed similar experiments, except T_{RM} were reactivated in the female reproductive tract (FRT) (Fig. 1f). Ex-T_{RM} appeared in blood within 10 days, and these cells bore marks reminiscent of mucosal T_{RM}, including slight underexpression of CD44 and Ly6C relative to circulating memory T cells (Fig. 1g). These observations suggest that T_{RM} cells exhibit migrational plasticity and undergo retrograde migration after re-stimulation.

It was previously reported that antigen rechallenge at barrier sites induced CD69$^+$ T_{RM} within draining lymph nodes and that these cells had emigrated from the upstream nonlymphoid tissue[28]. Here, we transferred naive P14 CD8$^+$ T cells to naive mice, and infected recipients with Lymphocytic choriomeningitis virus (LCMV, Armstrong strain) intraperitoneally (i.p.) the following day. This established memory P14 CD8$^+$ T cells throughout organism, including within the FRT[29]. 30 days later, we treated the mice with FTY720 for 8 days, which inhibits S1P-mediated cell egress[30]. On the second day of treatment, cognate gp33 peptide was delivered transcervically to reactivate local P14 memory CD8$^+$ T cells[27,31]. When draining iliac lymph nodes were assessed 30 days later, we observed a substantial reduction in CD69$^+$ LN T_{RM} cells in mice that were treated with FTY720 during T cell activation (Supplementary Fig. 1). These data suggest that S1P contributes to the egress of reactivated T cells from nonlymphoid tissues.

Epigenetic profiling of T_{RM} reveals memory state with potential developmental plasticity

We wished to compare the potential developmental plasticity of CD8$^+$ T_{RM} cells with other CD8$^+$ T cell lineages including naive, T_{CM} and T_{EM} cells. We focused on small intestine intraepithelial lymphocytes (SI IEL) T_{RM} because they are uniformly (>99%) resident after LCMV infection based on parabiosis studies[29]. Moreover, SI IEL T_{RM} express a highly differentiated T_{RM} phenotype (CD103$^+$, CD69$^+$, granzyme B$^+$, CD62L$^-$, Ly6C^{lo}, IL-1MP5Rb^{lo}), whereas CD8$^+$ T cells, including T_{RM} cells in other tissues, are more heterogeneous[22,32,33] (Fig. 2a). SI IEL T_{RM} also express CCR9 (Fig. 2a). To generate naive, early and late effector, and memory CD8$^+$ T cell subsets expressing identical TCRs, we

Author Manuscript Author Manuscript Author Manuscript Author Manuscript

transferred naive CD90.1$^+$ P14 CD8$^+$ T cells to naive C57BL/6J mice. The following day, mice were infected with 2×10^5 PFU LCMV Armstrong i.p., which causes an infection that is cleared within approximately one week[34]. Four and eight days later, effector cells were sorted into memory precursor cells (MPs, CD127^{hi}KLRG1^{lo}) and terminal effector cells (TEs, CD127^{lo}KLRG1^{hi}). Memory P14 were isolated from LN or spleen at least three months later and sorted into CD62L$^+$ (T_{CM}) and CD62L$^-$ (T_{EM}) subsets or were isolated from small intestine epithelium and sorted to ensure a uniform CD103$^+$CD69$^+$CD62L$^-$ Ly6C^{lo} (T_{RM}) phenotype. Naive CD62L$^+$ cells were sorted from LNs of naive CD90.1$^+$ P14 Tg mice.

The transcriptome of LCMV-specific P14 T_{RM} cells isolated from gut has previously been reported[35]. Principal component analysis (PCA) revealed that T_{CM} and T_{EM} cells were nearly identical and more similar to naive T cells than T_{RM} cells (published dataset reanalyzed in Fig. 2b), supporting the contention that T_{RM} cells represent a distinct cell type or lineage.

Transcriptional profiling indicates what genes are currently being transcribed by a cell population. However, it does not inform which genes have the potential to be expressed under changing conditions or as a result of external stimuli. For instance, mRNA profiling fails to capture key biological differences between resting naive and memory T cells, such as the ability to synthesize IFNγ rapidly in the event of antigen recognition[36]. Whole genome bisulfite sequencing (WGBS) indicates which genes have been silenced by DNA methylation. In other words, it provides a readout more closely aligned with gene expression potential, rather than an indication of which genes are actively undergoing transcription. We performed whole genome bisulfite sequencing (WGBS) on naive, T_{CM}, T_{EM}, and T_{RM} cell subsets (Fig. 2c). Because T_{RM} cells share phenotypic properties with effector T cells, as a basis of comparison we also analyzed recently primed MPs and TEs.

Principal component analyses (PCA) of genome wide CpG methylation status in naive, recently activated effector cells, T_{CM}, T_{EM}, and T_{RM} cells revealed that there was little variance in methylation status in the memory T cell subsets. Specifically, the T_{CM}, T_{EM}, and T_{RM} cell subsets clustered together in a separate cluster while naive cells and the recently activated effector subsets were in separate clusters (Fig. 2c). Supplementary Fig. 2a details the methylation status of several T_{RM} specific genes among the naive, effector, and memory T cell subsets. It should also be noted that even when effector cells were removed from PCA, all memory subsets clustered together and away from naive T cells (Supplementary Fig. 2b). These data suggest that although T_{RM} cells share some phenotypic signatures with recently activated effector T cells (Fig. 2a), they may be resting memory T cells at the epigenetic level and share commonalities with other resting memory T cell subsets, including T_{CM} cells.

To explore developmental potential, we subjected our WGBS methylation datasets to machine learning algorithms designed to assign relative plasticity among cell types[37]. Here naive T cells, which biologically exhibit the most multipotency, are assigned a score of 1. Exhausted CD8$^+$ T cells exhibit a plasticity score of close to zero, in keeping with numerous observations supporting senescence and little developmental potential. Here we found that

Author Manuscript Author Manuscript Author Manuscript Author Manuscript

the T_{RM} plasticity score was intermediate between that defined for T_{CM} and T_{EM}, raising the possibility that T_{RM} cells may not be as terminally differentiated as previously proposed. Recently activated cells had plasticity scores that were almost as high as T_{RM} at D4 but diminished by D8 (Fig. 2d). Interestingly, SI IEL have been shown to be seeded approximately 4 days after infection in this LCMV infection model, and by day 7, effector cell migration to the SI is significantly diminished[32]. Moreover, KLRG1$^+$ CD8$^+$ T cells (a subset usually associated with terminal differentiation) are largely incapable of differentiating into CD103$^+$ T_{RM} cells[38–40]. Although our PCA analysis, which was based on the DNA methylation status of the CD8$^+$ T cells, broadly segregates the effector subsets from the memory subsets, our machine learning-derived plasticity index supported the hypothesis that the developmental potential of T_{RM} cells (as well as T_{CM} cells) is more comparable to CD8$^+$ T cells that have not undergone terminal differentiation.

Transdifferentiation of T_{RM} into circulating memory T cell subsets

The results above (Fig. 1 and 2) raised the possibility that T_{RM} cells may have developmental plasticity rather than represent a terminal effector stage of differentiation. This concept had been explored years prior, but without sorting cells on T_{RM} markers, leaving interpretation subjective[32]. To address this question, 90 days after transfer of naive P14 CD8$^+$ T cells and LCMV infection, memory P14 cells were isolated from pooled lymph nodes and sorted into CD62L$^+$ (T_{CM}) or spleen into CD62L$^-$ (T_{EM}) cells. In addition, P14 were isolated from SI IEL and sorted to ensure a uniform CD103$^+$CD69$^+$CD62L$^-$Ly6C^{lo} (T_{RM}) phenotype (see Fig. 3a for pre- and post-sort analysis).

To directly test developmental plasticity, 20,000 sorted naive, T_{CM}, T_{EM}, or SI IEL T_{RM} P14 cells were transferred i.v. into separate naive C57BL/6J recipients (Fig. 3a). Mice were then infected with LCMV, and the primary or recall response from transferred memory cells was monitored in blood (Fig. 3b). We observed that CD62L was gradually upregulated at the population level in blood by all subsets except T_{EM} (Fig. 3c). Hierarchically, naive T cells most rapidly produced CD62L$^+$ memory T cell progeny, followed by T_{CM}, then T_{RM} cells (Fig. 3c and d).

These data indicate that after isolation and re-stimulation, purified bona fide SI IEL T_{RM} cells have the capacity to differentiate into T_{CM} cells. Consistent with T_{RM} developmental plasticity, we found that bloodborne secondary Ex-T_{RM} cells had downregulated CD69 and CD103 (Fig. 3e). However, it should be noted that we found phenotypic traces of their non-lymphoid history imprinted on circulating secondary Ex-T_{RM} cells: both Ly6C and CCR9 expression only slowly conformed to the canonical circulating phenotype, and even at the latest time point analyzed (100 days after re-stimulation), bloodborne secondary Ex-T_{RM} cells still exhibited phenotypic traces of their former tissue of residence (Fig. 3f and g).

Developmental plasticity and tissue redistribution of T_{CM} and T_{RM}

We next assessed the anatomic distribution of the progeny of transferred and re-stimulated T_{CM} and T_{RM} cells performed in Fig. 3. Again, primary memory T cells after transfer of naive P14 T cells was included as a basis of comparison. In spleen, T_{CM} cells produced more secondary memory CD8$^+$ T cells than did re-stimulated SI IEL T_{RM} cells. However,

Author Manuscript Author Manuscript Author Manuscript Author Manuscript

the progeny of intravenously transferred SI IEL maintained a predilection for repopulating the small intestine and were observed in both the lamina propria (SI LP) and epithelium by immunohistochemistry (Fig. 4a, b and d). This propensity did not extend to other T_{RM} compartments, such as salivary gland (SG) and FRT (Fig. 4a and b). Similar observations were made after transfer and recall of polyclonal endogenous N-specific $CD8^+$ T_{RM} cells isolated from SI IEL of VSV-infected mice (Supplementary Fig. 3). Accordingly, previous evidence suggested that T cells isolated from SG or lung retained a predilection for their tissue of origin[41,42].

If re-stimulated SI IEL returned to the small intestine, they retained the naive T cell-like capacity to acquire canonical site-associated residence signatures, including high expression of CD103 and CD69, and low expression of Ly6C (Fig. 4c). In contrast, T_{CM} progeny were moderately less likely to express CD103 and down regulate Ly6C. Secondary memory SI IEL that derived from transferred T_{RM} cells also maintained higher expression of Granzyme B long after clearance of LCMV Armstrong infection (Fig. 4c). These data indicate that although SI IEL T_{RM} exhibited developmental plasticity (Fig. 2), compared to T_{CM} cells they retain a bias to home to their parental tissue and reacquire SI IEL T_{RM} signatures.

Ex-T_{RM} remain epigenetically poised for migration and T_{RM} re-differentiation

To further test imprinting of memory T cell fates, we tested trans-generational developmental plasticity. First, P14 immune chimeras were generated as described in Fig. 3, which provided a source of flow sorted primary $CD90.1^+CD62L^+$ T_{CM} and $CD103^+CD69^+CD62L^-Ly6C^{lo}$ SI IEL T_{RM} cells. 20,000 of each population was transferred into separate recipients, followed by LCMV infection to induce a recall response. 100 days later, the secondary memory progeny of each population (referred to as 2º Ex-T_{CM} and 2º Ex-T_{RM}, respectively) were isolated from spleen (phenotype shown in Fig. 3e and Supplementary Fig. 4). 1×10^5 P14 cells (or 2.5×10^4 in some experiments) of each population were transferred to new naive recipient mice, these mice were infected with LCMV to induce a tertiary immune response, and the fate of donor cells was evaluated 50 days later. Primary memory cells and secondary Ex-T_{CM} cells provided a basis for comparison (Fig. 5a).

Tertiary Ex-T_{RM} cells retained properties of primary T_{RM} cells, even after proliferating and differentiating outside of the mucosa (as secondary Ex-T_{RM} cells were isolated from spleen). For instance, the population retained its predilection to repopulate the intestinal mucosal epithelium and to reacquire the phenotype observed among primary SI IEL T_{RM} cells (Fig. 5b-e). In contrast, tertiary Ex-T_{CM} cells increasingly deviated from the acquisition of a canonical SI IEL T_{RM} phenotype. These data imply that induction of a T_{RM} differentiation program during the primary response can influence subsequent fate upon recall, even when the cells are removed from the tissue where the residence program was acquired, and this program could be maintained through two generations of proliferation and transfer. In other words, these data indicate that a history of residence is epigenetically maintained despite the developmental plasticity of T_{RM} cells.

We further note that in the absence of reinfection upon transfer, neither secondary Ex-T_{RM} nor Ex-T_{CM} cells were recovered from the small intestine (Supplementary Fig. 5), consistent

Author Manuscript Author Manuscript Author Manuscript Author Manuscript

with a model whereby secondary Ex-T_{RM} cells require restimulation to migrate and re-differentiate into mucosal residents.

Ex-T_{RM} are poised to reacquire T_{RM} characteristics in response to cytokines

T_{RM} precursors are thought to differentiate in response to local cytokine cues encountered upon migration to nonlymphoid tissues[22,32,38,43]. Here, we compared the capacity of Ex-T_{RM}, Ex-T_{CM}, and Ex-T_{EM} cells (generated as in figure 3, except cells were isolated 70 days after secondary infection) to acquire T_{RM} signatures after culture with TGFβ, IL-2, and IL-15. Ex-T_{RM} cells were most poised to adopt SI IEL T_{RM} signatures in response to cytokines, including upregulation of CD69 and CCR9 and down regulation of Ly6C (Fig. 6a and b).

Discussion

Our data indicate that T_{RM} cells share more epigenetic signatures with circulating memory T cell subsets than recently activated effector T cells and furthermore, support a model by which T_{RM} cells express the memory-like qualities of anamnestic expansion, migration, and differentiation after antigen recognition. This contrasts with models that view T_{RM} as effector-like immediate responders that are terminally differentiated, with host recall responses relying on antigen dissemination to draining SLOs where anamnestic recall responses are induced solely by T_{CM} cells.

Primary immune responses can be considered ‘inside-out’, meaning they are induced in deeper tissues (e.g. LNs that drain barrier sites of infection), and then proliferate and migrate out towards infected tissues. This topology is likely compelled by adaptive immune systems that rely on extreme clonal diversity. Our data support the existence of ‘outside-in’ recall immune responses, whereby anamnestic responses are initiated and expand at frontline sites of infection and tissue barriers by local non-lymphoid T_{RM} cells[26,31], and form progeny that redistribute and even contribute to the circulating memory T cell pool. We speculate that this might provide some advantages for maintaining host protective immunity. For instance, in the event of reactivation, Ex-T_{RM} cells from SI IEL retained a bias to repopulate the intestinal mucosa and the capacity to reacquire T_{RM} signatures after arrival. In contrast, iterative re-stimulation of T_{CM} and Ex-T_{CM} cells resulted in populations of cells that lose T_{RM} differentiation capacity. Thus, in the event that T_{RM}-mediated front-line immunity wanes, or if an iterative environmental re-exposure were to exceed the capacity of local T_{RM} cells to contain the infection or antigen locally, previous exposures could have populated the circulating memory T cell compartment with cells predisposed to preferentially migrate back to the parent tissue and to re-establish local resident immunity. Such a process could better prepare the organism for defense against future reinfections. The fact that Ex-T_{RM} cells share minor phenotypic commonalities with their T_{RM} predecessors raises the possibility that analysis of blood could, in theory, give some indication of tissue-specific immunity.

This study demonstrates that naive T cells exhibit the greatest developmental plasticity, whereas both T_{CM} and T_{RM} cells bias against producing reciprocal subsets. However, this biasing is not absolute. T_{RM} cells are not terminally differentiated. And because both T_{CM} and T_{RM} cells can interconvert, it indicates that each subset is not a fixed discrete cell type

Author Manuscript Author Manuscript Author Manuscript Author Manuscript

or lineage, which rejects many models of memory T cell subset ontogeny, particularly those that define linear unidirectional subset relationships. We did note that SI IEL did not proliferate as well as T_{CM} cells upon i.v. transfer and reinfection. This might be due to extrinsic variables, for instance T_{RM} cells may not survive well or may not migrate to locations optimized for reactivation after isolation and transfer. These issues might be unphysiological products of experimental design. Alternatively, there may be cell intrinsic differences in activation and proliferation potential. Perhaps both intrinsic and extrinsic variables explain differences in observed T_{RM} and T_{CM} expansion.

As KLRG1 expression is sometimes associated with terminal T cell differentiation, our data is consistent with observations that T_{RM} derive from KLRG1^{lo} precursors[38,39]. That said, some contexts may not allow productive T_{RM} recall responses that expand the population, lead to a redistribution of T_{RM}, or reveal developmental plasticity, as reported for HSV-specific recall responses in mouse skin[25]. It is unclear whether these differences are related to HSV-specific memory or other aspects of site-specific immunity, but we previously found that VSV-specific memory T cells positioned in skin were capable of recall responses that expanded the local population[26].

It was previously observed that LN T_{RM} cells accumulate in regional lymph nodes after local reinfection[28]. We further demonstrated that LN T_{RM} cells derived from cells previously present in the upstream nonlymphoid tissue, and we showed evidence of retrograde migration. Whether these cells derived from either bona fide nonlymphoid T_{RM} cells or transient migrants was not concluded. It should also be noted that T cells can recirculate through nonlymphoid tissues[15,44–47]. Retrograde migration occurs from skin xenografts by CD4$^+$ T cells that retain T_{RM} markers[33,48]. As these cells were postulated to recirculate in the steady state (reenter skin from blood in the absence of intentional restimulation), it is unclear whether this phenomenon relates to the Ex-T_{RM} biology we describe, or rather indicates that nonlymphoid recirculating cells may retain some markers in common with residents[2,44–46]. Indeed both resident and recirculating memory CD4$^+$ T cells have been identified in skin[33,47]. CD69$^+$ T cells are increased in the blood of psoriatic arthritis patients and CD103$^+$ T cells appear in human celiac disease patients after in vivo challenge with gluten[49,50]. Our study raises the possibility that these phenomena may be accounted for by Ex-T_{RM} cells.

In summary, this study demonstrates that T_{RM} cells share key features of developmental and migration plasticity with circulating memory T cells, including T_{CM} cells. Further evidence indicates that Ex-T_{RM} cells may shape the circulating pool to be predisposed to mount site-specific recall responses that preferentially maintain T_{RM} redifferentiation capacity.

Materials and Methods

Mice

C57BL/6J female mice were purchased from The Jackson Laboratory and were maintained in specific-pathogen-free conditions at the University of Minnesota. CD90.1$^+$ P14, CD45.1$^+$ P14, CD90.1$^+$ OT-I, and CD45.1$^+$ OT-I mice were fully backcrossed to C57BL/6J mice and maintained in our animal colony. B6.SJL mice were purchased from JAX and bred in-house.

Author Manuscript Author Manuscript Author Manuscript Author Manuscript

All mice used were 6–10 weeks of age and used in accordance with the Institutional Animal Care and Use Committees guidelines at the University of Minnesota.

Adoptive transfers and infections

We generated P14 immune chimeras by transferring 5×10^4 naive CD90.1$^+$ or CD45.1$^+$ P14 T cells i.v. into naive C57BL/6J mice and infecting mice with 2×10^5 plaque-forming units (PFU) of LCMV (Armstrong strain) i.p. the following day. OT-I immune chimeras were generated by transferring $5X10^4$ naïve CD90.1$^+$ or CD45.1$^+$ OT-I CD8$^+$ T cells into naive C57BL/6J mice. Mice were infected with $1X10^6$ PFU Vesicular Stomatitis Virus expressing chicken ovalbumin (VSVova) i.v. the following day. For cell sorting experiments, memory and naive P14 CD8$^+$ T cells were sorted using fluorescently labeled CD45.1 (A20), CD8β (YTS156.7.7), CD62L (MEL-14), Ly6C (AL-21 and HK1.4), CD127 (SB/199), CD44 (IM7), CD69 (H1.2F3) and CD103 (M290) antibodies in a Becton Dickinson FACSAria II. Following sort purification, 2×10^4 memory and naive P14 cells were transferred i.v. to new C57BL/6J recipients, followed by infection with 2×10^5 PFU of LCMV Armstrong i.p. in the same day.

In vivo antibody treatment and T_{RM} reactivation

Circulating CD90.1$^+$ P14 CD8$^+$ memory T cells were depleted by injecting 0.75 to 1.5 μg of anti-CD90.1 antibody (HIS51, eBioscience) i.p. as previously described[27]. 4 days after administration of antibody, 2×10^5 CD45.1$^+$ P14 or CD45.1$^+$ OT-I memory lymphocytes from the spleen and lymph node were transferred i.v. into depleted mice. Local T_{RM} reactivation was performed by delivering 50 μg of gp33 peptide trans-cervically (t.c.) in a 30 μl volume by modified gel loading pipet[27]. To reactivate OT-I CD8$^+$ T_{RM} cells positioned in skin, a $2cm^2$ area of the flank skin was shaved and 0.5 μg of SIINFEKL peptide was applied using a tattoo gun as previously described[28]. PBS was used in control animals.

Intravascular staining, lymphocyte isolation and phenotyping

To discriminate intravascular from extravascular cells, we injected mice i.v. with biotin-conjugated anti-CD8α as described[51]. Three minutes after the injection, we sacrificed the mice and harvested tissues as described[52]. Isolated cells were stained with antibodies to CD45.1 (A20), CD8α (53–6.7), CD8β (YTS156.7.7), CD27 (LG.3A10), CD62L (MEL-14), Ly6C (AL-21 and HK1.4), CD127 (A7R34), CCR9 (CW-1.2), CD44 (IM7), CD69 (H1.2F3), CD103 (M290 or 2E7), CD90.1 (OX-7 or His51), CD122 (TM-β1), CD49a (Ha31/8), CX3CR1 (SA011F11), α4β7 (DATK32) and KLRG1 (2F1), all from BD Biosciences, Tonbo Biosciences, Biolegend or Affymetrix eBiosciences. LCMV-specific T cells were stained with fluorescently conjugated H-2D^b/gp33 MHC I tetramers. Ova-specific T cells were stained with fluorescently conjugated H-2K^b/SIINFEKL MHC I tetramers. Endogenous VSV-specific cells were stained with fluorescently conjugated H-2K^b/N MHC I tetramers. Allophycocyanin (APC) or Phycoerythrin (PE)-conjugated anti-Granzyme B (GB12 or GB11, Invitrogen) antibody intracellular staining was performed using the Cytofix/Cytoperm kit (BD Pharmigen) following manufacturer's instructions. Cell viability was determined with Ghost Dye 780 (Tonbo Biosciences). The stained samples were acquired on LSRII or LSR Fortessa flow cytometers (BD) and analyzed with FlowJo software (Treestar).

Author Manuscript Author Manuscript Author Manuscript Author Manuscript

Tissue freezing and Immunofluorescence

Murine tissue was harvested, embedded and sectioned as described[29]. Briefly, 7 μm tissue sections were obtained from frozen tissue blocks in a Leica CM1860 UV cryostat. The sections were stained with CD8β (YTS156.7.7, Biolegend) and CD45.1 (A20, Biolegend) as above. The collagen-IV signal was amplified using AF488 Bovine anti-goat IgG (Jackson ImmunoResearch). Microscopy was performed using a Leica DM6000 B microscope and images were analyzed in Adobe Photoshop CS6.

Skin transplant surgeries

Skin transplant was performed as described earlier[53]. CD90.1$^+$ OT-I immune chimeric mice skin was harvested. The recipient (infection matched CD45.1$^+$ OT-I immune chimeric mice) graft bed was prepared by removing a ~1 cm^2 piece of skin from the upper left flank. The donor skin was attached on to the graft site using silk sutures (Sofsilk, Covidien) and a band aid was used to keep the graft in place. The band aid and sutures were removed 7 days post-surgery and the graft was allowed to heal for at least 30 days before peptide recall.

Genomic methylation analysis

DNA was isolated from 50,000 FACS-purified P14 CD8$^+$ T cells per sample using the Qiagen DNeasy blood and tissue kit. Genomic DNA was bisulfite-treated using the Zymo Research EZ DNA methylation kit. Bisulfite-induced deamination of cytosine was used to determine the allelic frequency of cytosine methylation of the target genomic region[54].The PCR amplicon was cloned into the pGEM-T TA cloning vector (Promega) then transformed into XL10-Gold ultracompetent bacteria (Stratagene). Individual bacterial colonies were grown and the cloning vector was isolated and sequenced. Library preparation and sequencing for the generation of whole genome DNA methylation profiles of naive and memory CD8$^+$ T cell subsets (T_{CM}, T_{RM}, and T_{EM}) were performed using previously established protocols[13,55]. The M values for the 3,000 most variable CpG sites were used for hierarchical clustering and PCA analyses in RStudio (v1.0.136). The built-in R *prcomp* and *autoplot* functions were used to perform PCA.

Plasticity score calculation

To identify the methylation state of the CpG sites associated with the T cell multipotent potential, a supervised analysis was performed between the methylomes from 3 wild type naive and 2 wild type after exhausted (35 days post chronic LCMV infection) gp33-specific CD8$^+$ T cells (methylation difference >=0.6 and FDR<= 0.01). A minimum of 10,000 cells were used per sample to establish the whole-genome methylation profiles of naïve and exhausted T cells. These whole genome methylation profiles were then used for the machine learning approach to develop the multipotency index. This analysis resulted in identification of 598 CpGs sites that were hypomethylated in naive CD8$^+$ T cells compared to exhausted CD8$^+$ T cells. This set of CpGs was then used as an input to the one-class logistic regression to calculate the multipotency signature using naive samples[37,56]. Once the signature was obtained, it was then applied to naive, T_{CM}, T_{EM}, T_{RM}, day 4 MP and TE, and day 8 MP and TE CD8$^+$ T cell methylomes. Exhausted CD8$^+$ T cell and effector CD8$^+$ T cell profiles were obtained from previously published data sets[13,55]. The score was calculated as the dot

Author Manuscript Author Manuscript Author Manuscript Author Manuscript

product between the DNA methylation value and the signature. The score was subsequently converted to the [0, 1] range. Data sets with multipotency indices closer to 1 were more similar to naive cells.

Global transcriptome analysis

Previously published mouse $CD8^+$ T cell transcriptome data was downloaded from GEO(GSE70813)[35]. Principal Component Analysis (PCA) was performed with the naive, T_{EM}, T_{CM}, and gut T_{RM} data samples in this data set. The built-in R *prcomp* and *autoplot* functions were used to perform the PCA and a plot of the first two principal components, respectively in RStudio (v1.0.136). Differential gene expression between the naive and gut T_{RM} samples was assessed with DESeq2(v1.12.4) using HOMER's getDiffExpression.pl using a false discovery rate (FDR) of 5% and a log2 fold change of 2[57].

In vitro T_{RM} differentiation assays

2×10^4 primary memory CD45.1$^+$ P14 T_{CM} from macroscopic lymph nodes, T_{EM} from spleen, and T_{RM} from SI IEL were transferred i.v. into individual naive C57BL/6J recipients and infected with 2×10^5 PFU LCMV-Armstrong the same day. 50–70 days post infection, single cell suspensions from the spleen and all macroscopic lymph nodes except mesenteric were isolated and $CD8^+$ T cells were purified using a $CD8^+$ T cell Negative Isolation Kit (StemCell Technologies). Cells were cultured as described previously[58], with modifications. Briefly, purified cells were incubated in individual wells with 20 IU/mL rhIL-2 (R&D Systems) and 50 ng/mL rhIL-15 (R&D Systems) for 2 days, followed by 2 day incubation with 20 IU/mL rhIL-2 and 50 ng/mL rhTGFβ−1 (R&D Systems) in complete RP-10 (RPMI-1640 containing 10% heat inactivated FBS, 100 U/ml penicillin/streptomycin, 1× nonessential amino acids, 1× essential amino acids, and β-mercaptoethanol). Cells were analyzed after 4 days.

Statistics

Sample distribution was evaluated using the D'Agostino and Pearson omnibus normality test. Parametric tests (unpaired two-tailed Student's t-test for two groups and one-way or two-way ANOVA with Tukey's multiple comparison test for more than two groups as indicated) or nonparametric (two-tailed Mann-Whitney U test) were used when specified. All statistical analysis was done in GraphPad Prism (GraphPad Software Inc.).

Data availability

All original data are available from the corresponding author upon request.

Life Sciences Reporting Summary

Further information on experimental design can be found in the Life Sciences Reporting Summary.

Supplementary Material

Refer to Web version on PubMed Central for supplementary material.

Author Manuscript Author Manuscript Author Manuscript Author Manuscript

Acknowledgments

We thank the members of the Masopust laboratory and the University of Minnesota Center for Immunology for helpful discussions. Funded by National Institutes of Health grant R01AI084913 and Howard Hughes Medical Institute Scholars program (D.M.) and FAPESP-BEPE (2015/00680-7) fellowship (R.F).

References

1. Obar JJ, Khanna KM & Lefrançois L Endogenous Naive CD8+ T Cell Precursor Frequency Regulates Primary and Memory Responses to Infection. Immunity 28, 859–869 (2008). [PubMed: 18499487]
2. Picker LJ & Butcher EC Physiological and Molecular Mechanisms of Lymphocyte Homing. Annu. Rev. Immunol 10, 561–591 (1992). [PubMed: 1590996]
3. von Andrian UH & Mackay CR T-Cell Function and Migration — Two Sides of the Same Coin. N. Engl. J. Med 343, 1020–1034 (2000). [PubMed: 11018170]
4. Masopust D. & Soerens AG Tissue-Resident T Cells and Other Resident Leukocytes. Annu. Rev. Immunol 37, 521–546 (2019). [PubMed: 30726153]
5. Park CO & Kupper TS The emerging role of resident memory T cells in protective immunity and inflammatory disease. Nat. Med 21, 688–697 (2015). [PubMed: 26121195]
6. Reinhardt RL, Khoruts A, Merica R, Zell T. & Jenkins MK Visualizing the generation of memory CD4 T cells in the whole body. Nature 410, 101–105 (2001). [PubMed: 11242050]
7. Gebhardt T, Wakim LM, Eidsmo L, Reading PC, Heath WR & Carbone FR Memory T cells in nonlymphoid tissue that provide enhanced local immunity during infection with herpes simplex virus. (2009). doi:10.1038/ni.1718
8. Masopust D, Vezys V, Marzo AL & Lefrançois L. Preferential localization of effector memory cells in nonlymphoid tissue. Science 291, 2413–7 (2001). [PubMed: 11264538]
9. Champagne P, Ogg GS, King AS, Knabenhans C, Ellefsen K, Nobile M, Appay V, Rizzardi GP, Fleury S, Lipp M, Förster R, Rowland-Jones S, Sékaly R-P, McMichael AJ & Pantaleo G. Skewed maturation of memory HIV-specific CD8 T lymphocytes. Nature 410, 106–111 (2001). [PubMed: 11242051]
10. Stemberger C, Neuenhahn M, Gebhardt FE, Schiemann M, Buchholz VR & Busch DH Stem cell-like plasticity of naïve and distinct memory CD8+ T cell subsets. Semin. Immunol 21, 62–68 (2009). [PubMed: 19269852]
11. Farber DL, Yudanin NA & Restifo NP Human memory T cells: generation, compartmentalization and homeostasis. Nat. Rev. Immunol 14, 24–35 (2014). [PubMed: 24336101]
12. Sallusto F, Geginat J. & Lanzavecchia A. Central Memory and Effector Memory T Cell Subsets : Function, Generation, and Maintenance. Annu. Rev. Immunol 22, 745–763 (2004). [PubMed: 15032595]
13. Youngblood B, Hale JS, Kissick HT, Ahn E, Xu X, Wieland A, Araki K, West EE, Ghoneim HE, Fan Y, Dogra P, Davis CW, Konieczny BT, Antia R, Cheng X. & Ahmed R. Effector CD8 T cells dedifferentiate into long-lived memory cells. Nature 552, 404–409 (2017). [PubMed: 29236683]
14. Mueller SN, Gebhardt T, Carbone FR & Heath WR Memory T Cell Subsets, Migration Patterns, and Tissue Residence. Annu. Rev. Immunol 31, 137–161 (2013). [PubMed: 23215646]
15. Gerlach C, Moseman EA, Loughhead SM, Alvarez D, Zwijnenburg AJ, Waanders L, Garg R, de la Torre JC & von Andrian UH The Chemokine Receptor CX3CR1 Defines Three Antigen-Experienced CD8 T Cell Subsets with Distinct Roles in Immune Surveillance and Homeostasis. Immunity 45, 1270–1284 (2016). [PubMed: 27939671]
16. Vezys V, Yates A, Casey KA, Lanier G, Ahmed R, Antia R. & Masopust D. Memory CD8 T-cell compartment grows in size with immunological experience. Nature 457, 196–199 (2009). [PubMed: 19005468]
17. Shin H. & Iwasaki A. Tissue-resident memory T cells. Immunological Reviews 255 (1),165–181 (2013). [PubMed: 23947354]
18. Nguyen QP, Deng TZ, Witherden DA & Goldrath AW Origins of CD 4+ circulating and tissue-resident memory T-cells. Immunology 157, 3–12 (2019). [PubMed: 30897205]

Author Manuscript Author Manuscript Author Manuscript Author Manuscript

19. Szabo PA, Miron M. & Farber DL Location, location, location: Tissue resident memory T cells in mice and humans. Sci. Immunol 4, eaas9673 (2019).
20. Glennie ND, Yeramilli VA, Beiting DP, Volk SW, Weaver CT & Scott P. Skin-resident memory CD4+ T cells enhance protection against Leishmania major infection. J. Exp. Med 212, 1405–14 (2015). [PubMed: 26216123]
21. Kadoki M, Patil A, Thaiss CC, Brooks DJ, Pandey S, Deep D, Alvarez D, von Andrian UH, Wagers AJ, Nakai K, Mikkelsen TS, Soumillon M. & Chevrier N. Organism-Level Analysis of Vaccination Reveals Networks of Protection across Tissues. Cell 171, 398–413.e21 (2017).
22. Casey KA, Fraser KA, Schenkel JM, Moran A, Abt MC, Beura LK, Lucas PJ, Artis D, Wherry EJ, Hogquist K, Vezys V. & Masopust D. Antigen-independent differentiation and maintenance of effector-like resident memory T cells in tissues. J. Immunol 188, 4866–75 (2012). [PubMed: 22504644]
23. Cheroutre H. IELs: enforcing law and order in the court of the intestinal epithelium. Immunol. Rev 206, 114–131 (2005). [PubMed: 16048545]
24. Wakim LM, Waithman J, van Rooijen N, Heath WR & Carbone FR Dendritic cell-induced memory T cell activation in nonlymphoid tissues. Science 319, 198–202 (2008). [PubMed: 18187654]
25. Park SL, Zaid A, Hor JL, Christo SN, Prier JE, Davies B, Alexandre YO, Gregory JL, Russell TA, Gebhardt T, Carbone FR, Tscharke DC, Heath WR, Mueller SN & Mackay LK Local proliferation maintains a stable pool of tissue-resident memory T cells after antiviral recall responses. Nat. Immunol 19, 183–191 (2018). [PubMed: 29311695]
26. Beura LK, Mitchell JS, Thompson EA, Schenkel JM, Mohammed J, Wijeyesinghe S, Fonseca R, Burbach BJ, Hickman HD, Vezys V, Fife BT & Masopust D. Intravital mucosal imaging of CD8+ resident memory T cells shows tissue-autonomous recall responses that amplify secondary memory. Nat. Immunol 19, 173–182 (2018). [PubMed: 29311694]
27. Schenkel JM, Fraser KA, Vezys V. & Masopust D. Sensing and alarm function of resident memory $CD8^+$ T cells. Nat. Immunol 14, 509–13 (2013). [PubMed: 23542740]
28. Beura LK, Wijeyesinghe S, Thompson EA, Macchietto MG, Rosato PC, Pierson MJ, Schenkel JM, Mitchell JS, Vezys V, Fife BT, Shen S. & Masopust D. T Cells in Nonlymphoid Tissues Give Rise to Lymph-Node-Resident Memory T Cells. Immunity 48, 327–338.e5 (2018).
29. Steinert EM, Schenkel JM, Fraser KA, Beura LK, Manlove LS, Igyártó BZ, Southern PJ & Masopust D. Quantifying Memory CD8 T Cells Reveals Regionalization of Immunosurveillance. Cell 161, 737–49 (2015). [PubMed: 25957682]
30. Brinkmann V, Cyster JG & Hla T. FTY720: Sphingosine 1-phosphate receptor-1 in the control of lymphocyte egress and endothelial barrier function. American Journal of Transplantation 4, 1019–1025 (2004). [PubMed: 15196057]
31. Schenkel JM, Fraser KA, Beura LK, Pauken KE, Vezys V. & Masopust D. Resident memory CD8 T cells trigger protective innate and adaptive immune responses. Science 346, 98–101 (2014). [PubMed: 25170049]
32. Masopust D, Vezys V, Wherry EJ, Barber DL & Ahmed R. Cutting edge: gut microenvironment promotes differentiation of a unique memory CD8 T cell population. J. Immunol 176, 2079–83 (2006). [PubMed: 16455963]
33. Watanabe R, Gehad A, Yang C, Scott LL, Teague JE, Schlapbach C, Elco CP, Huang V, Matos TR, Kupper TS & Clark RA Human skin is protected by four functionally and phenotypically discrete populations of resident and recirculating memory T cells. Sci. Transl. Med 7, 279ra39 (2015).
34. Wherry EJ, Blattman JN, Murali-Krishna K, van der Most R. & Ahmed R. Viral persistence alters CD8 T-cell immunodominance and tissue distribution and results in distinct stages of functional impairment. J. Virol 77, 4911–27 (2003). [PubMed: 12663797]
35. Mackay LK et al. Hobit and Blimp1 instruct a universal transcriptional program of tissue residency in lymphocytes. Science 352, 459–63 (2016). [PubMed: 27102484]
36. Kersh EN, Fitzpatrick DR, Murali-Krishna K, Shires J, Speck SH, Boss JM & Ahmed R. Rapid demethylation of the IFN-gamma gene occurs in memory but not naive CD8 T cells. J. Immunol 176, 4083–93 (2006). [PubMed: 16547244]

Author Manuscript Author Manuscript Author Manuscript Author Manuscript

37. Malta TM et al. Machine Learning Identifies Stemness Features Associated with Oncogenic Dedifferentiation. Cell 173, 338–354.e15 (2018).
38. Mackay LK, Rahimpour A, Ma JZ, Collins N, Stock AT, Hafon M-L, Vega-Ramos J, Lauzurica P, Mueller SN, Stefanovic T, Tscharke DC, Heath WR, Inouye M, Carbone FR & Gebhardt T. The developmental pathway for CD103+ CD8+ tissue-resident memory T cells of skin. Nat. Immunol 14, 1294–1301 (2013). [PubMed: 24162776]
39. Sheridan BS, Pham Q-M, Lee Y-T, Cauley LS, Puddington L. & Lefrançois L. Oral Infection Drives a Distinct Population of Intestinal Resident Memory CD8+ T Cells with Enhanced Protective Function. Immunity 40, 747–757 (2014). [PubMed: 24792910]
40. Herndler-Brandstetter D, Ishigame H, Shinnakasu R, Plajer V, Stecher C, Zhao J, Lietzenmayer M, Kroehling L, Takumi A, Kometani K, Inoue T, Kluger Y, Kaech SM, Kurosaki T, Okada T. & Flavell RA KLRG1+ Effector CD8+ T Cells Lose KLRG1, Differentiate into All Memory T Cell Lineages, and Convey Enhanced Protective Immunity. Immunity 48, 716–729.e8 (2018).
41. Hofmann M. & Pircher H. E-cadherin promotes accumulation of a unique memory CD8 T-cell population in murine salivary glands. Proc. Natl. Acad. Sci. U. S. A 108, 16741–6 (2011). [PubMed: 21930933]
42. Teijaro JR, Turner D, Pham Q, Wherry EJ, Lefrançois L. & Farber DL Cutting edge: Tissue-retentive lung memory CD4 T cells mediate optimal protection to respiratory virus infection. J. Immunol 187, 5510–4 (2011). [PubMed: 22058417]
43. Skon CN, Lee J-Y, Anderson KG, Masopust D, Hogquist KA & Jameson SC Transcriptional downregulation of S1pr1 is required for the establishment of resident memory CD8+ T cells. Nat. Immunol 14, 1285–1293 (2013). [PubMed: 24162775]
44. Cahill RNP, Poskitt DC, Frost H. & Trnka Z. Two distinct pools of recirculating T lymphocytes: Migratory characteristics of nodal and intestinal T lymphocytes. J. Exp. Med 145, 420–428 (1977). [PubMed: 299882]
45. Mackay CR, Marston WL & Dudler L. Naive and memory t cells show distinct pathways of lymphocyte recirculation. J. Exp. Med 171, 801–817 (1990). [PubMed: 2307933]
46. Collins N, Jiang X, Zaid A, Macleod BL, Li J, Park CO, Haque A, Bedoui S, Heath WR, Mueller SN, Kupper TS, Gebhardt T. & Carbone FR Skin CD4+ memory T cells exhibit combined cluster-mediated retention and equilibration with the circulation. Nat. Commun 7, 11514 (2016).
47. Gebhardt T, Whitney PG, Zaid A, MacKay LK, Brooks AG, Heath WR, Carbone FR & Mueller SN Different patterns of peripheral migration by memory CD4+ and CD8+ T cells. Nature 477, 216–219 (2011). [PubMed: 21841802]
48. Klicznik MM, Morawski PA, Höllbacher B, Varkhande SR, Motley SJ, Kuri-Cervantes L, Goodwin E, Rosenblum MD, Long SA, Brachtl G, Duhen T, Betts MR, Campbell DJ & Gratz IK Human CD4+CD103+ cutaneous resident memory T cells are found in the circulation of healthy individuals. Sci. Immunol 4, eaav8995 (2019).
49. Diani M, Casciano F, Marongiu L, Longhi M, Altomare A, Pigatto PD, Secchiero P, Gambari R, Banfi G, Manfredi AA, Altomare G, Granucci F. & Reali E. Increased frequency of activated CD8+ T cell effectors in patients with psoriatic arthritis. Sci. Rep 9, 10870 (2019).
50. Han A, Newell EW, Glanville J, Fernandez-Becker N, Khosla C, Chien YH & Davis MM Dietary gluten triggers concomitant activation of CD4+ and CD8+ αβ T cells and γλ T cells in celiac disease. Proc. Natl. Acad. Sci. U. S. A 110, 13073–13078 (2013).
51. Anderson KG, Mayer-Barber K, Sung H, Beura L, James BR, Taylor JJ, Qunaj L, Griffith TS, Vezys V, Barber DL & Masopust D. Intravascular staining for discrimination of vascular and tissue leukocytes. Nat. Protoc 9, 209–222 (2014). [PubMed: 24385150]
52. Thompson EA, Beura LK, Nelson CE, Anderson KG & Vezys V. Shortened Intervals during Heterologous Boosting Preserve Memory CD8 T Cell Function but Compromise Longevity. J. Immunol 196, 3054–63 (2016). [PubMed: 26903479]
53. Silva KA & Sundberg JP Surgical methods for full-thickness skin grafts to induce alopecia areata in C3H/HeJ mice. Comp. Med 63, 392–7 (2013). [PubMed: 24210015]
54. Trinh BN, Long TI & Laird PW DNA Methylation Analysis by MethyLight Technology. Methods 25, 456–462 (2001). [PubMed: 11846615]

Author Manuscript Author Manuscript Author Manuscript Author Manuscript

55. Ghoneim HE, Fan Y, Moustaki A, Abdelsamed HA, Dash P, Dogra P, Carter R, Awad W, Neale G, Thomas PG & Youngblood B. De Novo Epigenetic Programs Inhibit PD-1 Blockade-Mediated T Cell Rejuvenation. Cell 170, 142–157.e19 (2017).

56. Sokolov A, Carlin DE, Paull EO, Baertsch R. & Stuart JM Pathway-Based Genomics Prediction using Generalized Elastic Net. PLOS Comput. Biol 12, e1004790 (2016).

57. Love MI, Huber W. & Anders S. Moderated estimation of fold changes and dispersion fro RNA-seq data with Deseq2. Genome Biol. 15, 550 (2014). [PubMed: 25516281]

58. Pallett LJ, Davies J, Colbeck EJ, Robertson F, Hansi N, Easom NJW, Burton AR, Stegmann KA, Schurich A, Swadling L, Gill US, Male V, Luong T, Gander A, Davidson BR, Kennedy PTF & Maini MK IL-2high tissue-resident T cells in the human liver: Sentinels for hepatotropic infection. J. Exp. Med 214, 1567–1580 (2017). [PubMed: 28526759]

Author Manuscript Author Manuscript Author Manuscript Author Manuscript

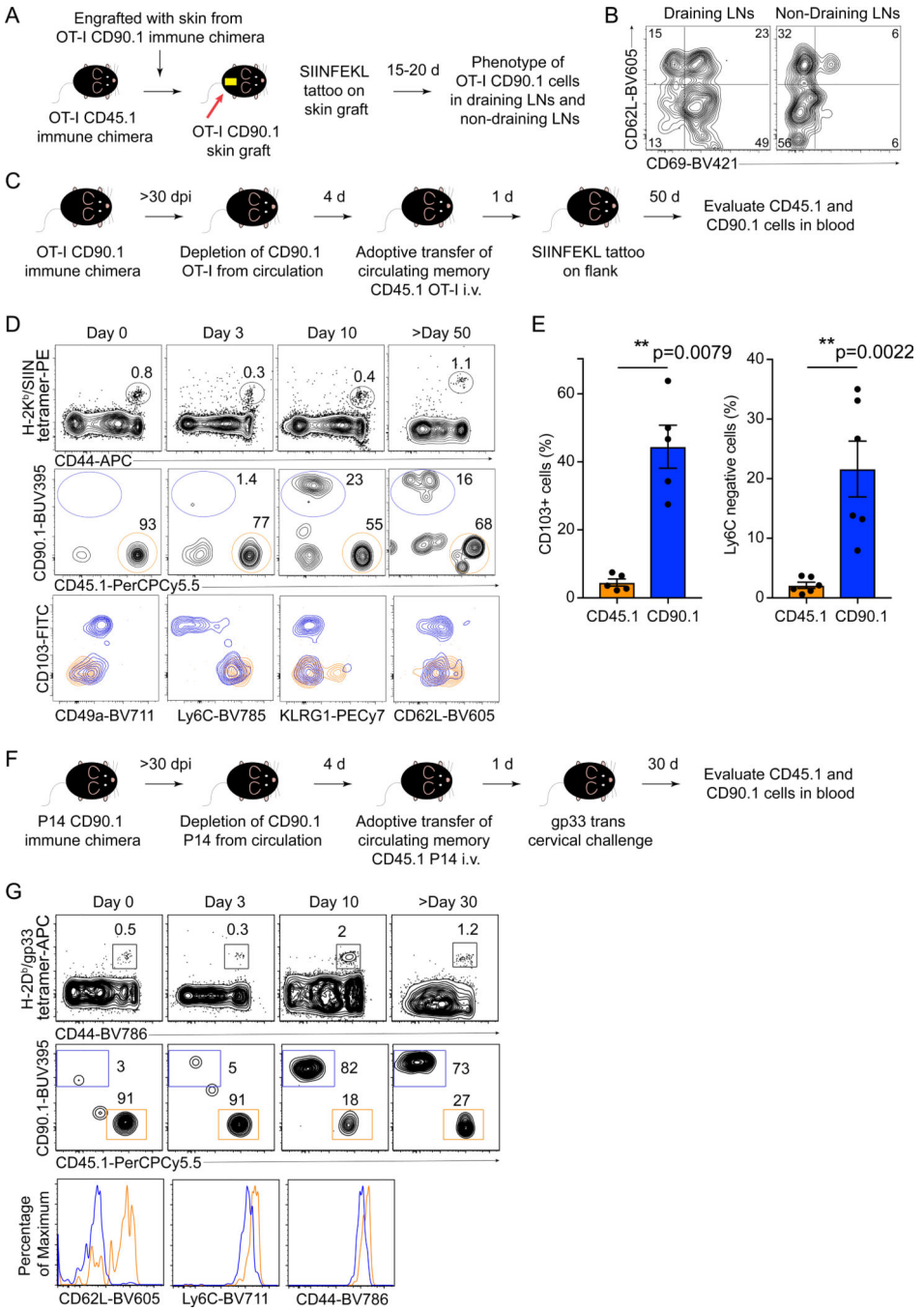

Fig 1. Local reactivation of T_{RM} precipitates egress to circulation.

a. Experimental design. **b.** Pooled draining and non-draining SLOs were used to phenotype the graft-derived CD90.1$^+$ OT-I T cells post reactivation. Gated on live CD90.1$^+$CD8α$^+$ T cells **c&d.** Experimental design and representative flow plots of H-2K^b/SIINFEKL tetramer$^+$ cells in the blood of mice after indicated days post-tattooing with SIINFEKL. Flow plots are gated on live CD8α$^+$ cells (top row) and H-2K^b/SIINFEKL tetramer $^+$, CD8α$^+$ T cells (middle row). Expression of CD103, CD49a, Ly6C, KLRG1 and CD62L was compared between CD45.1$^+$ (circulating memory derived, orange) and CD90.1$^+$ (resident memory

Author Manuscript Author Manuscript Author Manuscript Author Manuscript

derived, blue) cells 10 days post-recall in the bottom row. **e.** Bar graph depicting frequency of $CD103^+$ and $Ly6C^{lo}$ cells between $CD90.1^+$ and $CD45.1^+$ cells. Bars represent mean ± s.e.m and symbols represent individual animals. Two-tailed Mann-Whitney U test. **f&g.** Experimental design and representative flow plots of H-$2D^b$/gp33 $tetramer^+$ cells in the blood of mice after indicated days post t.c. challenge. Gated on live $CD8\alpha^+$ T cells (top row) and live H-$2D^b$/gp33 $tetramer^+$, $CD8\alpha^+$ T cells (middle row). Superimposed histograms of CD62L, Ly6C, and CD44 expression on $CD90.1^+$ (blue) and $CD45.1^+$ cells (orange) within the H-$2D^b$/$gp33^+$ specific population from blood 10 days post challenge. **b-g.** n=5 mice per experiment and one experiment shown of 3 independent experiments.

Author Manuscript Author Manuscript Author Manuscript Author Manuscript

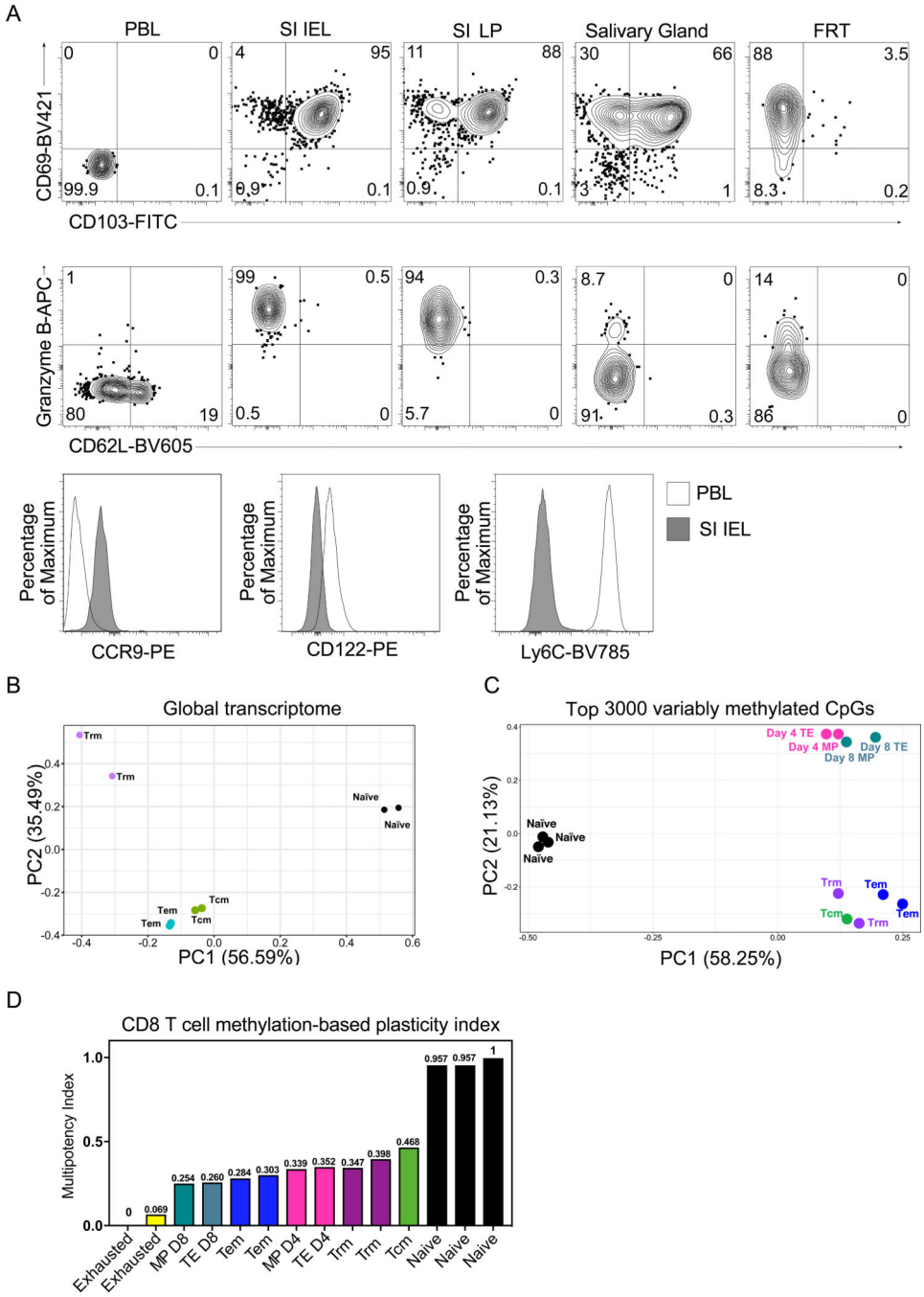

Fig 2. Epigenetic profiling of T_{RM} reveals memory state with potential developmental plasticity.

a. Representative phenotype of memory CD90.1^{+} CD8+ P14 cells isolated from the blood (PBL), epithelium (SI IEL) or lamina propria (SI LP) of the small intestine, salivary gland, or female reproductive tract (FRT) of LCMV immune chimeras 90 days after infection. Representative data of n=10 from two independent experiments. **b.** Principal Component Analysis (PCA) of previously published CD8^{+} naive, T_{CM}, T_{EM}, and gut T_{RM} transcriptome[35]. n=2 per group. **c.** CD8^{+} CD90.1^{+} P14 cells were isolated 4, 8, or 90 days after LCMV infection, and naive P14 cells were used for comparison. Spleen day 4 and 8

Author Manuscript Author Manuscript Author Manuscript Author Manuscript

effector populations were sorted into $CD127^{hi}KLRG1^{lo}$ (memory precursor, MP) or $CD127^{lo}KLRG1^{hi}$ (terminal effector, TE) populations. Memory populations were sorted into T_{CM} ($CD44^{+}CD127^{+}CD62L^{+}$, spleen), T_{EM} ($CD44^{+}CD127^{+}CD62L^{-}$, spleen), T_{RM} ($CD62L^{-}CD103^{+}CD69^{+}Ly6C^{-}$, SI IEL), and naive ($CD44^{-}CD127^{-}CD62L^{+}$, spleen). Whole genome bisulfite sequencing was performed to determine allelic frequency of cytosine methylation. Day 4 and day 8 effector P14 subset methylation data were obtained from a previously published study[13]. PCA of the top 3000 variably methylated CpGs in $CD8^{+}$ naive, day 4 and day 8 MP and TE, T_{CM}, T_{EM} and T_{RM}, each dot represents one sample from 50,000 cells. **d.** Hierarchical summary graph of $CD8^{+}$ T cell subset differentiation potential derived from a DNA methylation-based T cell multipotency index. CpG sites were identified from a machine learning algorithm using naive and exhausted gp33-specific CD8 T cells as a training data set. Plasticity indices were derived from the methylation status of 598 CpG sites. Each bar represents an individual sample.

Author Manuscript Author Manuscript Author Manuscript Author Manuscript

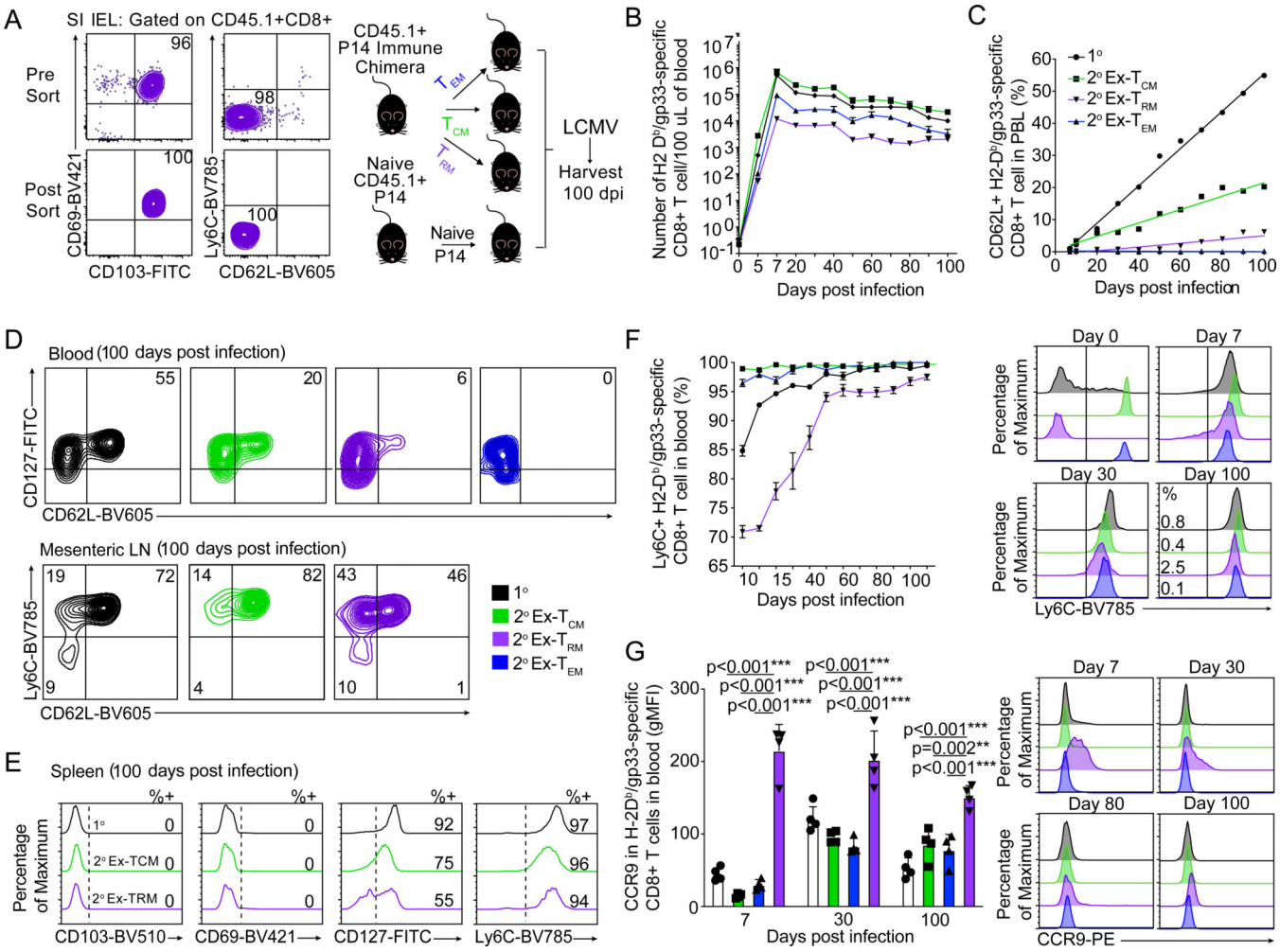

Fig 3. Transdifferentiation of T_{RM} into circulating memory T cell subsets.

$CD45.1^+$ P14 cells were isolated from LCMV immune chimeras 90 days after LCMV infection and sorted into T_{CM} ($CD8\alpha^+CD45.1^+CD44^+CD127^+CD62L^+$, isolated from pooled lymph nodes), T_{EM} ($CD8\alpha^+CD45.1^+CD44^+CD127^+CD62L^-$, isolated from spleen), and T_{RM} ($CD8\alpha^+CD45.1^+CD62L^-CD103^+CD69^+Ly6C^-$, isolated from SI IEL). 20,000 T_{CM}, T_{EM}, T_{RM}, and naive P14 cells were transferred into separate C57BL/6J recipients, which were subsequently infected with LCMV Armstrong. The recall response was monitored in blood until 100 days post infection, after which mice were sacrificed and tissues were analyzed. **a**. Post sort analysis of T_{RM} cells and experimental design. Number (**b)** and percent of $CD62L^+$ (**c**) of each transferred P14 $CD8^+$ T cell subset in blood over time. **d.** Representative FACS analysis of CD127, CD62L and Ly6C expression on transferred cells in blood or mesenteric LN 100 days after recall. **e.** Representative histograms of CD103, CD69, CD127 and Ly6C expression on transferred cells in spleen 100 days post transfer. **f.** Longitudinal Ly6C and **g.** CCR9 expression and representative histograms on P14 $CD8^+$ T cells. One-way ANOVA with Tukey's multiple comparison test. **b, f.** Symbols represent mean ± s.e.m. **c.** Symbols represent mean with linear regression line. **g.** Bars represent mean ± s.e.m. and symbols represent individual mice. **b-g.** n=4 mice per

group per experiment and data are representative of 1 of 4 independent experiments with similar results.

Author Manuscript Author Manuscript Author Manuscript Author Manuscript

Author Manuscript Author Manuscript Author Manuscript Author Manuscript

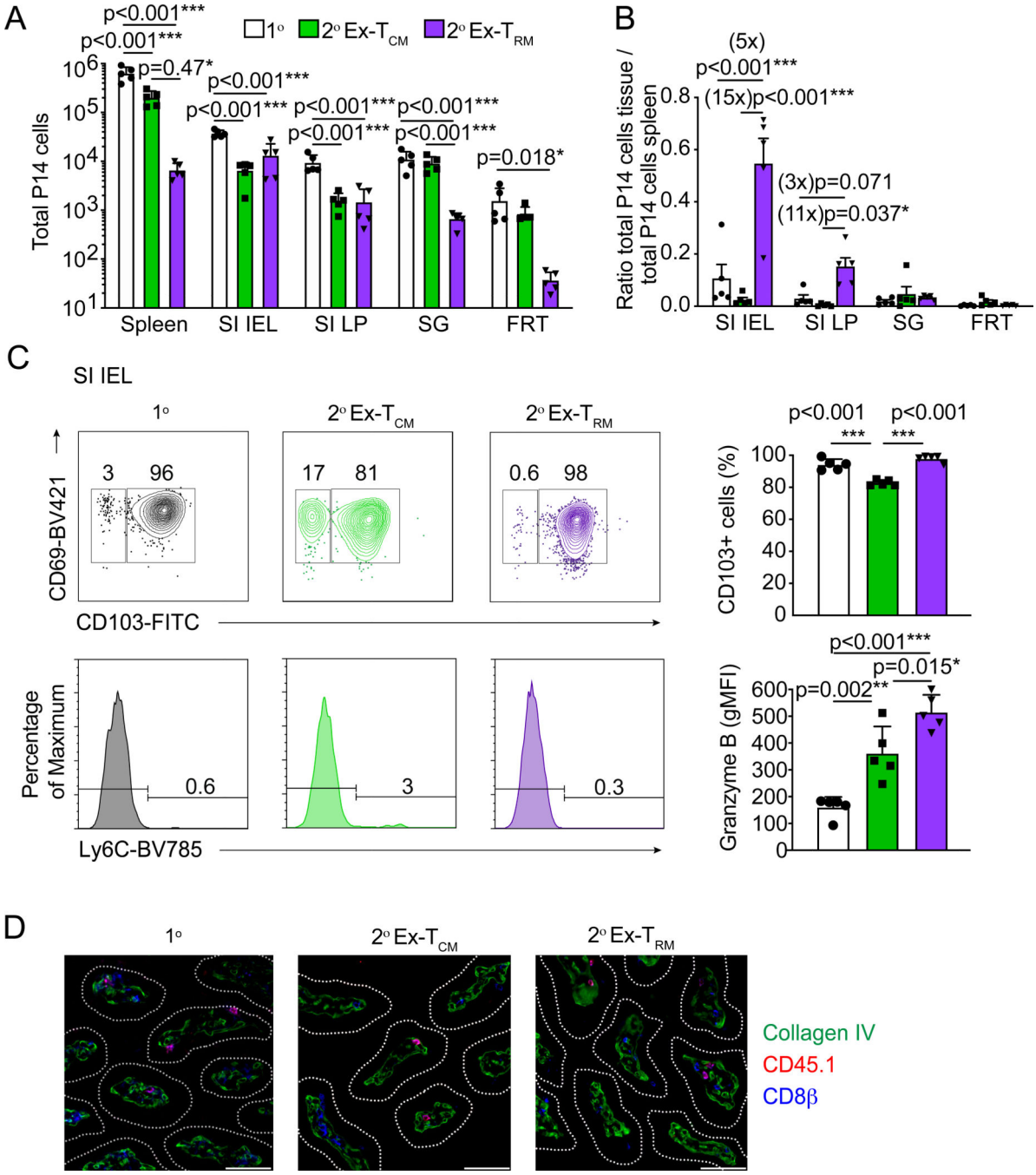

Fig 4. Developmental plasticity and tissue redistribution of T_{CM} and T_{RM}

. a. Recovery of P14 cells from transferred T_{CM}, T_{RM} and naive (as in Fig. 3) in spleen, SI IEL, SI LP, salivary gland (SG) and female reproductive tract (FRT) 100 days after recall. **b.** Ratio of P14 cells in spleen to either SI IEL, SI LP, SG and FRT. **c.** CD69, CD103, Ly6C and Granzyme B expression on transferred cells recovered from SI epithelium after 100 days after recall. Gated on i.v.$^-$, CD8β$^+$, CD44$^+$, CD45.1$^+$, H-2D^b/gp33 tetramer$^+$. **d.** Representative immunofluorescence images of SI. Scale bars, 50 microns. **a-c**. One-way ANOVA with Tukey's multiple comparison test. Bars represent mean ± s.e.m. and symbols

represent individual mice. **a-d.** n=5 mice per group per experiment and one shown of four independent experiments with similar results.

Author Manuscript Author Manuscript Author Manuscript Author Manuscript

Author Manuscript Author Manuscript Author Manuscript Author Manuscript

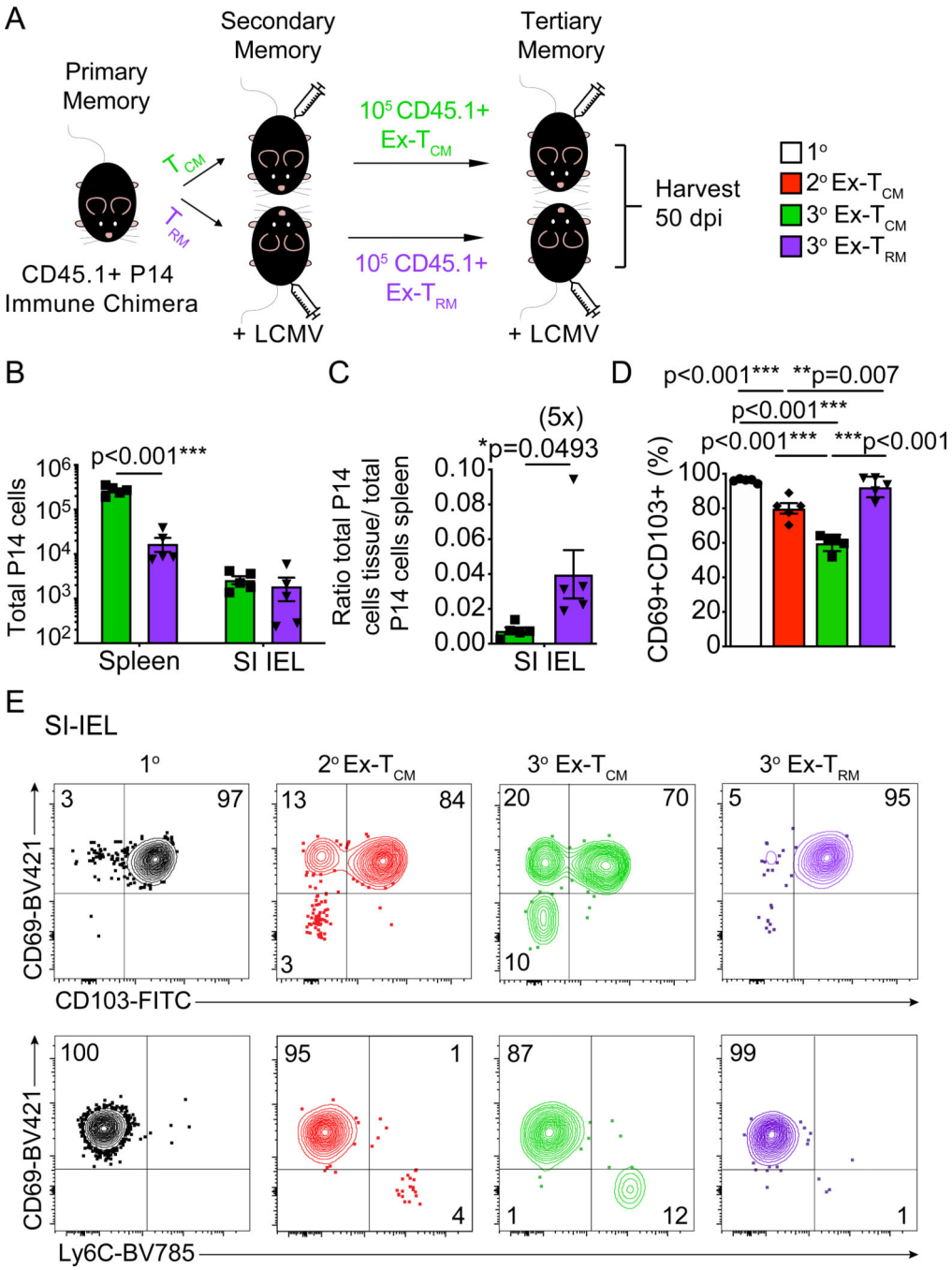

Fig 5. Ex-T_{RM} remain epigenetically poised for migration and T_{RM} re-differentiation.

a. 1° memory T_{CM} from LN and T_{RM} from SI IEL were sorted (as in Fig. 3) and transferred to naive recipients, followed by LCMV infection. 100 days later, splenocytes containing 10^5 2° memory P14 were transferred to naive recipients, again followed by LCMV infection. 50 days later, 3° memory P14 were analyzed for phenotype and distribution. 1° and 2° responses were assessed for comparison in **d** and **e**. **b.** 3° memory P14 isolated from spleen and SI IEL. Multiple unpaired two-tailed Student's t-test. **c.** Ratio of 3° memory P14 isolated from SI IEL to spleen. Unpaired two-tailed Student's t-test. **d, e.** Percentage of $CD69^+CD103^+$ 3°

Author Manuscript Author Manuscript Author Manuscript Author Manuscript

memory P14 cells and **r**epresentative plots of CD69, CD103 and Ly6C expression on P14 isolated from SI IEL. 3º Ex-T_{CM} and Ex-T_{RM} were compared to 1º and 2º Ex- T_{CM} mucosal memory. Gated on i.v.$^{-}$, CD8β^{+}, CD44^{+}, CD45.1^{+}, H-2D^{b}/gp33 tetramer^{+}. One-way ANOVA with Tukey's multiple comparison test. **b-e**. Bars represent mean ± s.e.m. and symbols represent individual mice. n=5 mice per group per experiment and one shown of two independent experiments with similar results.

Author Manuscript Author Manuscript Author Manuscript Author Manuscript

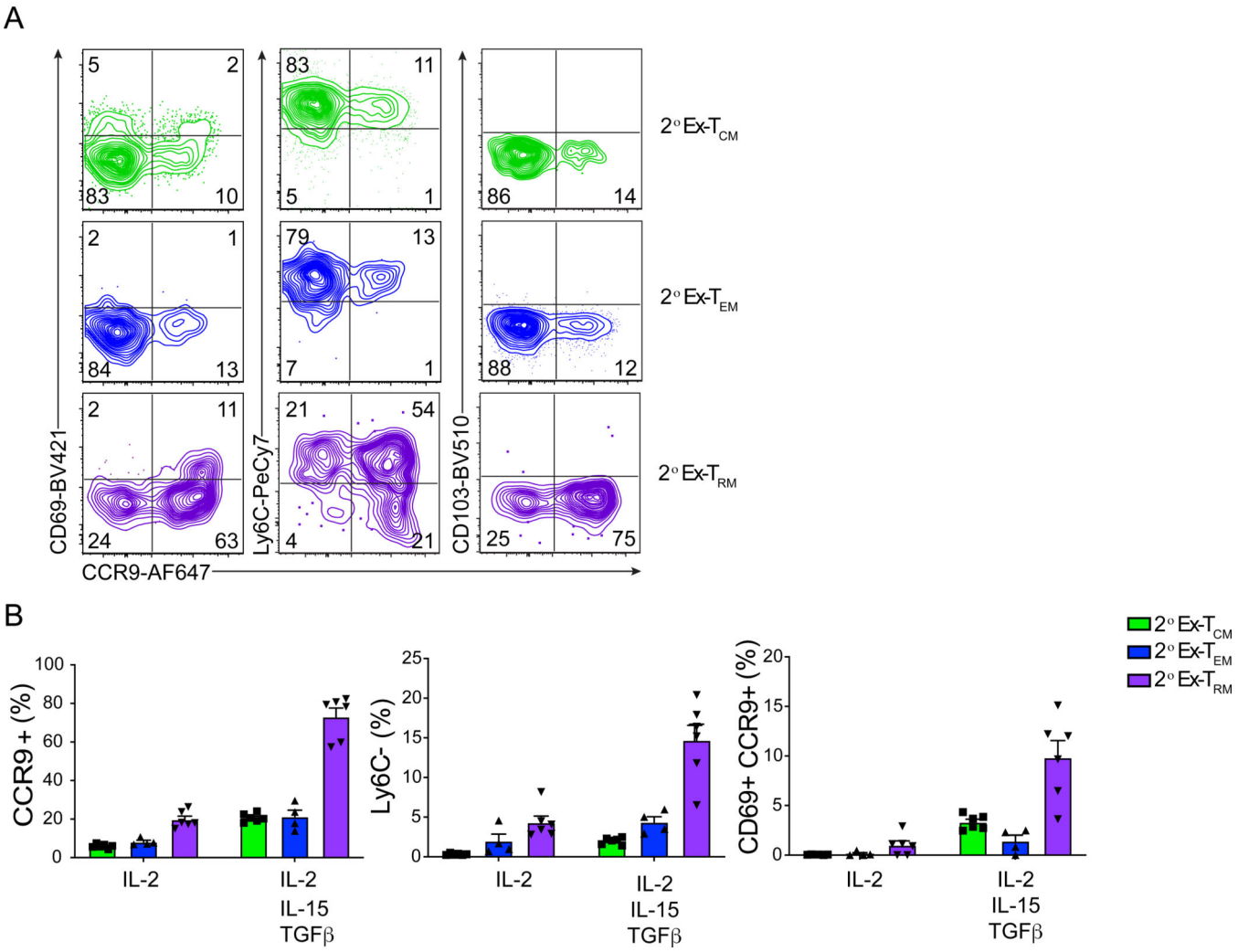

Fig 6. Ex-T_{RM} are poised to reacquire T_{RM} characteristics in response to cytokines.

1° memory T_{CM} from LN, T_{EM} from spleen, and T_{RM} from SI epithelium were sorted (as in Fig. 3) and transferred to naive recipients which were subsequently infected with LCMV-Armstrong. 50–70 days post infection, splenocytes were isolated and progenies of each cell subtype were stimulated in vitro with IL-15 and TGFβ to induce T_{RM}-biased differentiation program. IL-2 was included in all cultures. Cells were analyzed after four days in culture. **a.** Representative flow plots and **b.** summary of IL-15, TGFβ and IL-2 stimulated cultures and gated on H-2D^b/gp33 tetramer$^+$, CD45.1$^+$, CD8α$^+$ T cells. T_{CM}, T_{RM} (n=6 technical replicates per group) and T_{EM} (n=5 technical replicates) from 3 pooled mice per group are shown from one of two independent experiments with similar results.